Lipid Composition and the Lateral Pressure Profile in Bilayers

Robert S. Cantor
The Department of Chemistry, Dartmouth College, Hanover, New Hampshire 03755 USA

ABSTRACT The mechanisms by which variations in the lipid composition of cell membranes influence the function of membrane proteins are not yet well understood. In recent work, a nonlocal thermodynamic mechanism was suggested in which changes in lipid composition cause a redistribution of lateral pressures that in turn modulates protein conformational (or aggregation) equilibria. In the present study, results of statistical thermodynamic calculations of the equilibrium pressure profile and bilayer thickness are reported for a range of lipids and lipid mixtures. Large redistributions of lateral pressure are predicted to accompany variation in chain length, degree and position of chain unsaturation, head group repulsion, and incorporation of cholesterol and interfacially active solutes. Combinations of compositional changes are found that compensate with respect to bilayer thickness, thus eliminating effects of hydrophobic mismatch, while still effecting significant shifts of the pressure profile. It is also predicted that the effect on the pressure profile of addition of short alkanols can be reproduced with certain unnatural lipids. These results suggest possible roles of cholesterol, highly unsaturated fatty acids and small solutes in modulating membrane protein function and suggest unambiguous experimental tests of the pressure profile hypothesis. As a test of the methodology, calculated molecular areas and area elastic moduli are compared with experimental and simulation results.

INTRODUCTION

Variations in the lipid composition of cell membranes can strongly affect the behavior of membrane proteins. The underlying interactions between bilayer components (lipids or other membrane-soluble molecules) and proteins can be distinguished on the basis of "specificity": the former can influence the latter either through direct binding to localized protein sites, or indirectly, by altering the structural, thermodynamic, or dynamic properties of the bilayer, which in turn modulates protein behavior. Certainly, there are many systems, particularly involving peripheral membrane proteins, in which the presence of a specific lipid submolecular fragment is crucial to protein function, strongly suggesting local recognition and binding; such interactions are not considered in the present study. Rather, we examine the consequences of a putative nonspecific mechanism of lipid modulation of protein conformational equilibria and peptide aggregation (Cantor, 1997a, 1997b). These equilibria are often sensitive to variation of lipid molecular characteristics, such as head group repulsion and the length or degree of unsaturation of the hydrocarbon tails, or to the concentrations of cholesterol and smaller solutes such as alcohols, general anesthetics, and other drugs. Examples of such sensitivity are well known (Bienvenüe and Sainte Marie, 1994): the nicotinic acetylcholine receptor, a ligand-gated excitatory ion-channel protein, does not function in the absence of cholesterol in the membrane (Rankin et al., 1997); the meta-I to meta-II transition in rhodopsin is activated by the presence of dodecahexaenoic acyl chains and enhanced by short alkanols (Brown, 1997; Litman and Mitchell, 1996); and the aggregation of alamethicin (the number of peptides in the pore-forming oligomer) has been shown to be lipid-dependent (Keller et al., 1993).

At present, the physical underpinnings of the nonspecific mechanisms by which membrane components influence embedded proteins are largely unknown. Proposed mechanisms have involved correlations of variations in bilayer composition with altered structural properties of the membrane (Bloom et al., 1991) such as thickness, coupled to the free energy through hydrophobic mismatch (Mouritsen and Bloom, 1993) or directly to thermodynamic properties such as microphase separation (Mouritsen and Jørgensen, 1997; Edidin, 1997; Holopainen et al., 1997) that can effect the free energy change of protein conformational equilibria. Curvature elastic stress is likely to play an important role in view of the considerable experimental evidence that proper membrane function requires incorporation of "nonlamellar" lipids (which, when the only lipid present, form inverse hexagonal phases) and that membrane homeostasis may involve proximity to the lamellar/hexagonal transition (Seddon, 1990; Brown, 1997; deKruijff, 1997; Andersson et al., 1998; Morein et al., 1996; Dan and Safran, 1998; Gruner, 1989; Gruner, 1991; Hui, 1997). Reviews can be found in a special issue of *Chemistry and Physics of Lipids* (Epand, 1996). Of particular interest is the coupling between hydrophobic mismatch and curvature stress, which has recently been carefully examined (Nielsen et al., 1998).

Whereas small variations in lipid composition can influence protein activity significantly, the accompanying changes in membrane structural properties such as thickness are typically small, although it has been argued that relatively small changes in thickness can have a significant effect on protein equilibria (Lundbaek and Andersen, 1999;

Received for publication 19 October 1998 and in final form 3 February 1999.

Address reprint requests to Robert S. Cantor, Department of Chemistry, Dartmouth College, Hanover, NH 03755. Tel.: 603-646-2504; Fax: 603-646-3946; E-mail: rcantor@dartmouth.edu.

0006-3495/99/05/2625/15 $2.00

Nielsen et al., 1998). However, such structural changes can often be achieved by small variations in temperature or other external variables that have relatively little effect on proteins (Franks and Lieb, 1994). In addition, the composition of a membrane can be varied in such a way as to maintain, for example, constant membrane thickness but which nonetheless has a significant effect on protein function, suggesting that other, nonstructural properties may play a major role in lipid modulation of protein activity.

In recent work (Cantor, 1997a, 1997b) a simple thermodynamic argument has been suggested that provides a mechanistic link between changes in the lateral pressure profile (the depth-dependent distribution of lateral stresses within the membrane) and protein conformational (or aggregation) equilibria for those intrinsic membrane proteins whose function involves a structural change accompanied by a depth-dependent variation in the cross-sectional area of the protein in the transmembrane domain. Using statistical mechanical methods, it was shown that the redistribution of pressures accompanying biologically significant changes in lipid composition could plausibly result in significant shifts in protein conformational equilibria. The methodology used to predict these shifts involved a simplified lattice approach, and results were presented only for membranes comprised of lipids whose chains were of uniform flexiblity, corresponding to saturated chains. In the present study, the statistical mechanical approach has been extended and refined to incorporate details of key lipid characteristics. These calculations allow prediction of effects of varying chain length and unsaturation, head group repulsions, and incorporation of cholesterol and small interfacially active solutes (alcohols, general anesthetics) on the pressure profile and on membrane thickness.

As discussed above, it seems likely that maintaining constant thickness is important, presumably, to ensure hydrophobic matching with intrinsic proteins. Addition of cholesterol or increasing chain length causes membrane thickening, whereas increased chain unsaturation or the strength of head group repulsions causes the bilayer to thin. In the right proportions, certain combinations are predicted to leave the thickness unchanged while radically altering the lateral pressure profile, thus separating effects of hydrophobic mismatch from redistributions of lateral stresses.

It is important to note that the influence of the lateral pressure distribution is not only intimately related to but underlies the effects of curvature stress in protein function. For small membrane deformations, the curvature elastic characteristics are expressed through the spontaneous curvature and the splay and Gaussian curvature elastic moduli (bending stiffnesses). As is well known, these parameters, which completely determine the curvature dependence of the free energy, derive from integral moments of the pressure profile and its curvature derivative. From the fact that 1) curvature elastic properties (evidenced for example by proximity to a hexagonal/lamellar transition) are closely related to 2) lipid modulation of protein behavior one can not conclude that the former causes the latter. Rather, it may only indicate that both have a common physical origin, the lateral pressure profile.

The theoretical methodology is described in the second section, summarized where it is identical to the approach of earlier study, whereas the extensions and refinements are presented in detail. It should be stressed that the qualitative character of most of the results is not affected by the details of the calculational methodology. The reader more interested in the predictions can pass directly to the third section, in which the results of calculations (pressure profiles, molecular areas, and area elastic moduli) are presented and compared for a range of lipid composition, and related, at least qualitatively, to known effects of lipid compositional changes on protein function. These predictions suggest an unambiguous test of the proposed mechanism, which would require that different lipid compositions engineered to have similar pressure profiles should lead to similar protein function, whereas those lipid mixtures that alter the pressure profile should result in significantly modified protein behavior that depends directly on the specific changes in the pressure profile.

THEORETICAL APPROACH

A mean-field statistical thermodynamic theory is used to calculate the equilibrium properties of the lipid bilayer system, using a lattice model to describe the chain conformational contributions to the free energy. The utility of this kind of methodology for predicting structural and thermodynamic properties has been demonstrated for a variety of aggregates formed by flexible surfactants in solution, as well as self-assembled and spread monolayer and bilayer films (Ben-Shaul, 1995; Ben-Shaul and Gelbart, 1994; Leermakers and Lyklema, 1992; Wijmans et al., 1994; Leermakers and Scheutjens, 1988; Cantor, 1995, 1996.)

Lattice model

The methodology in the present study derives from that developed to describe amphiphilic monolayers at an oil/water interface (Cantor, 1993, 1996), appropriately modified to model lipid bilayers. As with all models, it relies on assumptions and approximations that serve to make the calculations tractable and result in interpretable predictions. The bilayer is treated as two compact monolayers, in each of which the segments of the acyl chains occupy space at constant bulk density, i.e., no "free volume" is permitted. The distribution of chain segments is described using a lattice model in which a chain configuration is defined as occupying a particular set of contiguous lattice sites. As in previous studies, the boundary between the hydrophilic (head-group) region and hydrophobic interior of the bilayer is approximated by a sharp planar interface. By constraining the junction of each acyl chain with its head group to reside on that plane, the complexity of, for example, the glycerol/carbonyl linkage between the phosphocholine head group

and the acyl tails in phospholipids is completely ignored as is the considerable roughness present in the interfacial region (Merz and Roux, 1996; Tielemann et al., 1997). Although interfacial roughness could readily be incorporated into the model (Leermakers and Scheutjens, 1988), it would require assumptions about additional interaction energies that are not well known, so it is unlikely that any further predictive value would obtain. In the cubic lattice, the sites can be grouped into layers labeled $i = 1, \ldots, h$ by proximity to the aqueous (or head-group) interface. Layer 1 represents the sites in contact with the aqueous/head group region, whereas the contact between layers h of the two monolayers occurs across the bilayer midplane. For simplicity of calculation, it is assumed that chains do not cross the bilayer midplane, i.e., there is no interdigitation between monolayers. (This restriction certainly causes an increase in the fraction of bonds oriented horizontally near the midplane, affecting the orientational ordering and the lateral pressure in that region. For most biological membranes, there is little interdigitation, so this approximation is expected to be of minor importance. However, for some combinations of lipids, such as mixtures of flexible chains of very different lengths, interdigitation may occur to a much greater extent, neglect of which may lead to significant errors in predictions of properties that depend sensitively on the chain orientational distribution, such as the pressure profile.) The z axis is assigned to the bilayer normal, so the x and y axes define the bilayer plane. If δz is the thickness of a layer of lattice sites, then $H = (\delta z)h$ represents the thickness of the monolayer.

Chain bond orientations

In principle, the bond between one chain segment and the next along the chain backbone can be oriented in any direction, defined by the continuum of solid angles. For purposes of enumeration, this continuum is divided up into a set of discrete directions each subtending a fraction of the total solid angle. In the cubic lattice, there are six lattice sites adjacent to a site in layer i: in layers $i + 1$ and $i - 1$ along the "vertical" z axis, and two in each of the "horizontal" directions (x and y) in layer i. A chain conformation is described by the set of contiguous lattice sites (and associated bonds along the x, y, and z axes between them) to which it most closely corresponds.

Chain flexibility and structure

For saturated polymethylenic chains, an internal energy cost is associated with the formation of a 90° bend in the cubic lattice. The assignment of a numerical value to this energy is somewhat arbitrary because there is no simple relation between rotational isomeric states of polymethylenic chains (and the associated energy difference between trans and gauche conformers) and cubic lattice conformational states. However, comparison with predictions of chain end-to-end distances in polyethylenic chains and with the predicted surface densities of bilayer aggregates restricts the values to a fairly narrow range. *Cis*-unsaturation is most simply (if crudely) modeled as a strong energetic preference for a 90° bend at the point of unsaturation. The distribution of the volume of cholesterol is described as follows. Because its cross-sectional area is (roughly) twice that of an all-trans hydrocarbon chain, each cholesterol molecule is modeled as a pair of rigid rods, one end of each localized to the aqueous interface. Although the fused ring structure is rigid, the backbone axis can tilt to some extent away from the bilayer normal. However, as the cubic lattice is not good at modeling rigid rods (allowing only vertical and horizontal orientations) we compensate by allowing slight flexibility in the fused ring portion of the cholesterol molecule. On the opposite end of one rod is attached one end of a hydrocarbon tail assumed to have the same flexibility as used to describe saturated acyl chains.

Free energy

The configurational entropy of the flexible chains is calculated in mean-field approximation, incorporating bond-correlated excluded volume, as in previous studies. We let A represent the average surface area per chain with corresponding dimensionless surface area $a = A/A_0$, in which A_0 is the area of a lattice site face. Because the system is constrained such that all sites are occupied by a single chain segment, the thickness of the monolayer (h) is related to the chain length (i.e., the volume per chain in units of lattice site volume) through $a = n/h$, thus ensuring that each layer has the same volume (number of sites).

The probability of different conformational states q is designated as $P(q)$. Each segment of each conformation q is characterized by the layer i in which it is found and the orientation D of the bond from the preceding segment along the chain. Because of the inhomogeneity of the bilayer in the z direction, it is important to distinguish between the positive and negative z directions; we thus define $D = x, y, +z$, and $-z$. The numbers of such segments for a given configuration q are given by $\phi_{D,i}(q)$, and the average obtained from a sum over the probability distribution $\phi_{D,i} = \Sigma_q \phi_{D,i}(q) P(q)$. The average number of segments (dimensionless volume) per chain in layer i, independent of direction, is given by $\phi_i = \Sigma_D \phi_{D,i}$. For a completely "filled" bilayer, the system will be constrained such that $\phi_i = a$ for all layers i.

The entropy of each monolayer is calculated as in earlier studies through the following procedure. A large number N of amphiphiles, with some (as yet undetermined) conformational probability distribution, is successively placed on the lattice, the segments placed sequentially starting from the head group junction. For each molecule, the number of available sites for the first segment is multiplied for each of its remaining segments by the probability that the lattice site into which it is to be placed is unoccupied. There are various

levels of approximation at which this probability can be determined; as discussed elsewhere (Cantor, 1996; Cantor and McIlroy, 1989; Leermakers and Scheutjens, 1988; Leermakers and Lyklema, 1992), it is important to use a mean-field approximation of excluded volume that accounts for bond orientational correlations. It is useful to define a set of bond directions $d = x$, y, and v, in which $b_{d,i} = \phi_{d,i}$ for $d = x$, y, and for the vertical direction (all bonds between layers i and $i + 1$) $b_{v,i} = \phi_{+z,i+1} + \phi_{-z,i}$. As shown in previous work (Cantor, 1993, 1996), after a fraction $\theta = j/N$ of chains has already been placed in the monolayer, the probability for successful placement in layer i of a particular segment of the next ($j + 1^{st}$) chain is given by $f_i/g_{x,i}$, $f_i/g_{y,i}$, $f_i/g_{v,i-1}$, and $f_i/g_{v,i}$, for segments placed in the x, y, $+z$, and $-z$ directions, respectively, in which $f_i(\theta) = 1 - \theta a^{-1}\phi_i$ is the fraction of unoccupied sites in layer i, and $g_{d,i}(\theta)$ corrects for bond orientational correlations, with $g_{d,i} = 1 - \theta a^{-1} b_{d,i}$. Using this expression for the segment placement probabilities, it is possible to evaluate (in mean-field approximation) the number of distinguishably different resulting arrangements of the monolayer once all N molecules have been placed ($\theta = 1$). In the thermodynamic limit of a large number of chains, an expression for the conformational entropy per chain is obtained as an explicit function of a and the chain probability distribution $P(q)$:

$$S/k_B = \ln a - \sum_q [P(q) \ln P(q)] + a \sum_i \sum_d g_{d,i} \ln g_{d,i} \quad (1)$$

It is straight-forward to obtain a corresponding expression for a mixture of molecules of different types (e.g., lengths or stiffnesses). Let $m = 1, 2, \ldots$, label each such molecule, of length n_m, expressed in units of the size of a lattice site. We let χ_m represent the mole fractions of the different acyl chain types. The average chain length is then $n = \Sigma_m \chi_m n_m$, and the segment distribution is given by

$$\phi_{D,i} = \sum_m \chi_m \sum_q \phi_{D,i}(q_m) P(q) \quad (2)$$

and the entropy can be written as

$$S/k_B = -\sum_m [\chi_m \ln \chi_m] + \ln a - \sum_m \chi_m \sum_q [P(q_m) \ln P(q_m)] + a \sum_i \sum_d g_{d,i} \ln g_{d,i} \quad (3)$$

Bilayer energy

As in previous studies, we consider three contributions to the internal energy of the bilayer: chain energies (comprising bending stiffness and possibly a local attraction of some segments for the aqueous interface), interfacial tension, and head group electrostatic interactions. For each chain component k, an energy $\epsilon_{b,k}$ (dimensionless, in units of k_BT) is defined for a 90° bend between successive bonds relative to that for collinear bonds. (As described below, chains with 180° bends are not allowed.) For saturated, i.e., single-bonded methylene groups, $\epsilon_{b,s} \approx 1$; for *cis*-unsaturation, i.e., for the single bond following a *cis*-double bond it is very negative, $\epsilon_{b,u} \ll -1$, and for rigid linear rods, $\epsilon_{b,r} \gg 1$. The dimensionless internal energy of each chain state is taken as the sum of the local bending energies: $\epsilon_b(q_m) = \Sigma_k n_k(q_m)\, \epsilon_{b,k}$. The average bending energy per chain is thus $e_b = \Sigma_m \chi_m \Sigma_q P(q_m)\, \epsilon_b(q_m)$.

The energy of the aqueous interface of each monolayer is assumed to be proportional to the area of nonbonded interface between the hydrophobic and hydrophilic regions, i.e., the average dimensionless interfacial energy per chain is γa, to within an additive constant. This approximation is equivalent to assuming a constant interfacial tension γ, equal to that at the interface between water and bulk hydrocarbon, localized to the interfacial plane.

We model head group interactions in a quasi-two-dimensional mean-field approximation consistent with our development of the chain conformational entropy. We thus assume that the head groups are distributed randomly (subject to excluded volume, i.e., a step-function radial distribution) within a plane located on the aqueous side of the interface. The resulting contribution to the average energy per chain e_{hg} (dimensionless, in units of k_BT) is proportional to the fraction of chains with interacting head groups, their surface density, and the strength of the pair potential between nearest neighbors, so that $e_{hg} = u_{hg}\, \chi_{hg}^2 a^{-1}$. The constant u_{hg} (dimensionless, in units of k_BT) can be estimated from measured pressure-area isotherms and deduced virial coefficients for spread monolayer films (Stigter et al., 1992), by comparison of lipids with strongly interacting head groups, such as phosphatidylcholine (PC), with lipids whose head groups that have much weaker electrostatic interactions such as phosphatidylethanolamine (PE). From those results, we obtain $u_{hg}(\text{PC}) \approx 5.0$ at 25°C (the value increasing rapidly with temperature), and $u_{hg} \approx 0$ for PE and the hydroxyl "head group" in cholesterol and alcohols. Because there are two chains per head group, a system comprised entirely of PC lipids has $\chi_{hg} = 0.5$, whereas a mixture of PC with lipids without interacting head groups has $\chi_{hg} < 0.5$. Incorporation of all contributions to the free energy F yields

$$F/k_BT = \gamma a + u_{hg} a^{-1} - \ln a + \sum_m [\chi_m \ln \chi_m] + \sum_m \chi_m \sum_r \{P(r_m) \ln [P(r_m)/\zeta(r_m)]\} - a \sum_i \sum_d g_{d,i} \ln g_{d,i} \quad (4)$$

in which $\xi(r_m) = \Sigma_q \exp[-\epsilon_b(q_m)]$ is the statistical weight of the set of conformations $\{q_m\} \in r_m$ having the same segment and bond distribution $n_k(q_m)$, as an explicit function of the molecular area and the chain probability distribution. In prior studies on spread monolayer films at the oil/water interface, the probability distribution was determined by minimizing the free energy subject to a normalization constraint on the sum of the probabilities. For bilay-

ers at (approximately) constant density, i.e., in which the sites are assumed to be completely filled, the average number of sites occupied per chain must be constrained to be equal to the area per chain:

$$\phi_i - a = 0 \quad i = 1, \ldots, h-1 \tag{5}$$

For given average chain length, the area per chain is set to ensure an integral number of layers of the same volume. Thus, one of the layer constraints may be eliminated, so we only explicitly constrain the volume in the first $h-1$ layers. Minimization of the free energy with respect to each $P(r_m)$, for each chain type m, using Lagrange multipliers ζ_i for each of the constraints of Eq. 5, and one for the probability normalization, leads to an explicit expression for the probabilities:

$$P(r_m) = \Lambda(r_m)/Q_m \tag{6}$$

$$\Lambda(r_m) = \xi(r_m)\prod_i \left\{ \exp[-\phi_i(r)\lambda_i] \prod_d \exp[-b_{d,i}(r) \ln g_{d,i}] \right\}$$

in which $\lambda_h = 1$, $\lambda_i = 1 - \zeta_i$ for $1 \le i \le h-1$, and the configurational partition function for chains of type m is given by $Q_m = \Sigma_r \Lambda(r_m)$. Using these probabilities, the dimensionless free energy $f = F/k_BT$ can be written as

$$f = \gamma a + u_{hg}a^{-1} - a\sum_i \sum_d g_{d,i} \ln g_{d,i} - \sum_i \phi_i\lambda_i - \sum_m \chi_m \ln (Q_m a/\chi_m) \tag{7}$$

This expression for the free energy cannot yet be evaluated because the values of $g_{d,i}$ and λ_i are not yet determined. Each $g_{d,i}$ depends on the chain probabilities, which in turn are explicit functions of the entire set of $g_{d,i}$ and λ_i. For given thickness h (and thus molecular area a), these values can be determined by reiterative solution of a set of equations for the directional segment distributions $\phi_{D,i}$ as given in Eq. 2. In each layer i, initial guesses are made for the $\phi_{+z,i}$ and $\phi_{-z,i}$ (except in layer h, for which $\phi_{-z,i} = 0$, and for layer 1, in which $\phi_{+z,i} = 1$) and for λ_i in layers $i = 1$ to $h-1$. The constant volume constraint then determines $\phi_{x,i}$ ($= \phi_{y,i}$) in each layer, because $\phi_{x,i} = \phi_{y,i} = [a - (\phi_{+z,i} + \phi_{-z,i})]/2$. These guesses are used to determine the $g_{d,i}$, which then allows evaluation of the chain probability distribution from which new values of the $\phi_{D,i}$ are obtained. The procedure is performed reiteratively using a generator matrix method (Cantor, 1996) until convergence is reached; it is checked with varying initial guesses to ensure that the solution is unique.

In all calculations for which results are presented below, we have used a value of $\gamma = 2.5$, corresponding to an interfacial tension of $2.5(k_BT/A_0) \approx 50$ dyn/cm, a representative value (Jaycock and Parfitt, 1981) at the fluid interface between medium length alkanes and water. We set $A_0 \approx 20$ Å^2, the approximate area per chain of a fluid monolayer of vertically aligned (all-trans) hydrocarbon chains. The thickness of a layer is taken to be $\delta z \approx 1.27$ Å, the length of a methylene group along the director of an all-trans chain. Unfortunately, this results in a lattice in which the sites are not isodiametric, being considerably smaller in the vertical than in the horizontal directions. This broken symmetry affects the description of the chain conformational statistics, but it can largely be accounted for by appropriate choice of the bending (free) energy. In the present study, we (somewhat arbitrarily) set $\omega = \exp(-\epsilon_b/k_BT) = 0.45$ for a 90° bend of a saturated alkyl chain. Calculations using this value yield approximately the correct end-to-end distance of alkyl chains in the melt and also predict the experimentally determined average molecular areas and number of kinks in lipid bilayers. Changes in the value of ω within physically reasonable limits alter the details of the predictions; decreasing ω leads to smaller molecular areas, greater chain orientational order, etc. However, qualitative features, such as the dependence of pressure profiles on chain unsaturation, length, cholesterol content, etc., are independent of the choice of ω within a reasonable range.

Lateral pressures and equilibrium

The molecular area (and thus the thickness) of the equilibrium state of the bilayer occurs when the free energy is minimized with respect to area, i.e., when the lateral pressure $\Pi = -dF/dA$ is zero, or expressed in dimensionless units: $\pi = -df/da = -(A_0/k_BT)\Pi = 0$. Unfortunately, as mentioned above, the relationship between average area per chain and chain length ($ah = n$) permits only a discrete set of values of a for which the bilayer thickness is an integral multiple of the layer thickness, i.e., for which each compact monolayer has an integral number of layers completely filled with chain segments. The expression for the free energy in Eq. 7 is thus valid only for these discrete values of a, so it is not possible to determine the lateral pressure from an analytical derivative of this expression. To determine the equilibrium molecular area, we repeat the procedure described above for a range of different integral values of h and thus of a. The calculated values of f are plotted as a function of a and fit to a polynomial, the minimum of which determines both the equilibrium area a_{eq} and free energy f_{eq}. Typically, the discrete calculated free energies are found to be accurately fit by a quadratic (or at most a cubic) in a or $\ln(a)$. The calculated f_{eq} and a_{eq} are generally quite insensitive to the number of points or to the order of the polynomial used for the fit. The (nonintegral) number of layers at equilibrium is designated as h_{eq}, and the equilibrium thickness is thus given by $H_{eq} = h_{eq}\,\delta z = (h-1)\delta z + \delta z_h$, in which δz_h is the thickness of layer h.

An estimate for the lateral pressure distribution π_i (the lateral pressures in each layer i) at a_{eq} is obtained using the following approximation. For each value of a corresponding to an integral number of completely filled layers, we calculate the explicit areal derivative of the bilayer free energy, $\pi_c = -df/da$ (in dimensionless units), subject to the density constraints in layers 1 through $h-1$. This corresponds to the

procedure of increasing the area (the volume, at fixed thickness of the layer) in layers 1 through $h - 1$ by an amount dA, and decreasing it by an amount $(h - 1)dA$ in layer h. Of course, a decrease in area at fixed thickness of layer h is not equivalent to the physical effect of a decrease in thickness at fixed area, but it yields a reasonably good approximation, because the chains in this layer are typically quite disordered, and the pressure is small in this layer regardless of how it is approximated. In any case, this procedure allows the total lateral pressure π as well as the individual layer pressures π_i to be estimated. The quality of the approximation can be estimated by comparing π_c obtained by this procedure to the value for π determined from the best-fit $f(a)$ curves as described above, at each value of a. In most cases, the differences are predicted to be small (often smallest near the predicted free-energy minimum), and it is likely that the errors introduced are small compared with other approximations in the approach.

Setting the pressure equal to the negative of the areal derivative of the free energy of Eq. 7, subject to the $h - 1$ constraints given in Eq. 5, leads to the following simple expression for π_c, the calculated (dimensionless) pressure:

$$\pi_c = -\gamma + \pi_{hg} + \sum_i \pi_i \tag{8}$$

in which the head group contribution is $\pi_{hg} = u_{hg}\, a^{-2}$, and the layer pressures are given by

$$\pi_i = \lambda_i + \ln g_{x,i} + \ln g_{y,i} + \ln g_{v,i} \quad (1 \le i \le h - 1)$$

$$\pi_h = 1 + \ln g_{x,h} + \ln g_{y,h}$$

The equilibrium head group pressure is calculated directly, with $\pi_{hg,eq} = u_{hg}\, a_{eq}^{-2}$. An estimate for the pressure $\pi_{i,eq}$ in layer i at the equilibrium area a_{eq} is obtained by interpolating between the values of π_i calculated for the pair of areas a' and a'' (with corresponding pressures π' and π'') that bracket a_{eq}: $\pi_{i,eq} = (\pi_i'\pi'' - \pi_i''\pi')/(\pi'' - \pi')$. Use of the weighting factors π' and π'' ensures that the total pressure is zero at equilibrium. In many cases, a plot of π_i against area is found to be nearly linear, so this procedure provides a reasonably good approximation.

RESULTS

Predicted lateral pressure profiles are presented for systems of varying lipid composition. In all cases studied here, the two monolayers of the bilayer are of identical composition. Thus, in the pressure profiles, only half of the bilayer is shown. For purposes of graphing the pressures as an explicit function of depth in the bilayer (z), the pressure of a layer is localized at the value of z corresponding to the center of that layer. As discussed in previous work (Cantor, 1997b), it is useful to reexpress $\pi(z)$ as a lateral pressure density $p(z) = \pi(z)/\delta z$, which is independent of the choice of layer thickness, for sufficiently small δz. (In the limit $\delta z \to 0$, the number of layers becomes infinite, so the pressure at given depth must tend to zero in proportion to δz, and the value of $p(z)$ at given z is thus independent of the layer thickness.) In units of bulk pressure, $p(z)$ is obtained from the (dimensionless) lateral pressure $\pi(z)$ through $p(z) = p_0\, \pi(z)$, in which $p_0 = k_B T/(A_0 \delta z)$, except in layer h, in which δz is replaced by the fractional thickness δz_h.

There is an intrinsic difficulty in comparing $p(z)$ for bilayers comprised of different lipids because their predicted equilibrium thicknesses will generally differ. Because it is clearly impossible to align, for example, both aqueous interfaces among bilayers of different thickness, a single bilayer position must be selected. There are two obvious (if arbitrary) choices. It is often useful to align the aqueous interface of one monolayer and report the depth (z) as distance therefrom; for example, to consider variations in the pressure experienced by a small amphiphilic solute that will likely be localized near the aqueous interface. It is also useful to display the pressures by aligning the center of the bilayer, in which case z represents the distance from the bilayer center; this may be more useful in considering effects of shifts in the pressure profile on transmembrane proteins.

Single-component bilayers

In the first set of results, presented in Fig. 1, we examine single-component bilayers of varying chain length and unsaturation, considering first lipids without head-group electrostatic interactions ($u_{hg} = 0$). (Note that the area under the $p(z)$ curve represents the sum of all but the interfacial tension contribution to the total pressure and is thus constant for $u_{hg} = 0$.) The effect of increasing chain length from 14 to 20 carbons in saturated lipids is presented in Fig. 1 (center-aligned in panel a and interfacially-aligned in panel b). Not surprisingly, increasing length results in progressively larger bilayer thickness and molecular area, as seen in Table 1. The pressure density is predicted to decrease as it spreads out over the half of the monolayer adjacent to the bilayer center, whereas the pressure profile within the first few layers adjacent to the aqueous interface shows little dependence on chain length. The effect of varying position of a single *cis*-double bond for 18-carbon chains is presented in Fig. 1*c* and *d*. For chains with *cis*-unsaturation close to the terminal methyl, such as $18{:}1_{\Delta 15}$, the pressure profile is very similar to that obtained for the saturated 18:0, because the double bond is distributed fairly broadly around the bilayer center where the chains are quite orientationally disordered even without the *cis*-double bond. As the location of the *cis*-unsaturation is moved up the chain toward the head group, the effect on the pressure profile becomes more pronounced. For $18{:}1_{\Delta 12}$, the membrane thins and the pressure increases slightly, mostly in the middle of the monolayer. For $18{:}1_{\Delta 9}$, the decrease in bilayer width is much greater and the more pronounced pressure increase is maximal closer to the aqueous interface, although it is still broadly distributed. Moving the double bond closer to the

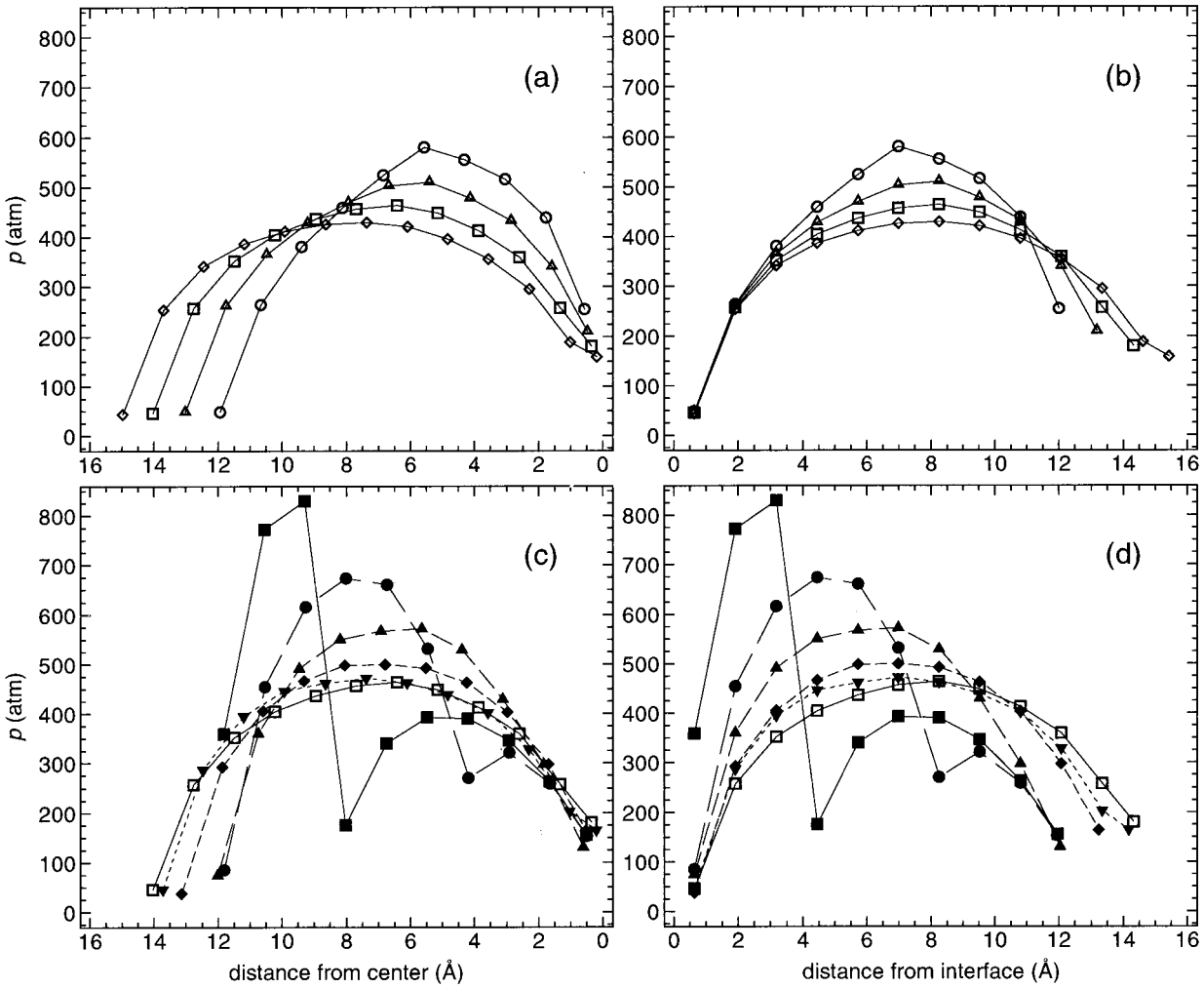

FIGURE 1 Lateral pressure profile of single-component bilayers without head group repulsions. As in all figures, only one-half of the (symmetric) profile is shown. Individual points are located at the center of the layer over which the pressure is exerted; connecting lines are included as a guide to the eye. Panels (*a*) and (*c*) are center-aligned ($z = 0$ at the center), whereas (*b*) and (*d*), containing the same data as in (*a*) and (*c*), respectively, are interfacially-aligned ($z = 0$ at the interface). Saturated lipids: (○) 14:0; (△) 16:0; (□) 18:0; (◇) 20:0. Singly *cis*-unsaturated 18-carbon lipids: (▼) $18{:}1_{\Delta 15}$; (◆) $18{:}1_{\Delta 12}$; (▲) $18{:}1_{\Delta 9}$; (●) $18{:}1_{\Delta 6}$; (■) $18{:}1_{\Delta 3}$.

interface leads to qualitative changes in the pressure profile, although the thickness of the bilayer is not further reduced. For $18{:}1_{\Delta 6}$ and particularly for $18{:}1_{\Delta 3}$, the double bond is necessarily localized near the aqueous interface, resulting in the very large excess pressure. The larger molecular area causes the chains to be much more orientationally disordered nearer the center of the bilayer, leading to a decrease in pressure. It is useful to compare the trends resulting from increased length of saturated chains and the position of chain unsaturation. Note that while both a decrease in length and a shift of the double bond away from the methyl terminus toward the middle of the chain lead to a broad pressure increase, it occurs in somewhat different region; in the former case toward the bilayer center and in the latter case more toward the aqueous interface.

It is important to examine the effect of multiple unsaturation at fixed chain length, because in addition to oleic acid ($18{:}1_{\Delta 9}$), the lipids formed from linoleic ($18{:}2_{\Delta 9,12}$), α-linolenic ($18{:}3_{\Delta 9,12,15}$), and γ-linolenic ($18{:}3_{\Delta 6,9,12}$) acids are important as precursors of arachidonic ($20{:}4_{\Delta 5,8,11,14}$) and docosahexaenoic ($22{:}6_{\Delta 4,7,10,13,16,19}$) acids, although the 18:3 fatty acids themselves are not commonly found in more than trace amounts in membranes. The predicted pressure profiles for $18{:}1_{\Delta 9}$, $18{:}2_{\Delta 9,12}$, and $18{:}3_{\Delta 9,12,15}$ are very similar, as seen in Fig. 2*a*, i.e., starting with a double bond at the middle of the chain, there is little effect upon incorporation of additional *cis*-unsaturation progressively toward the methyl terminus. As seen in Table 1, the bilayer thickness is also little changed. This suggests that, to the extent that the pressure profile influences membrane function, these three lipids may be largely interchangeable. This is not the case if the unsaturation begins closer to the head group. The effects of $\Delta 6$ and $\Delta 9,12$ unsaturation are somewhat additive, as seen in Fig. 2*b* and Table 1. The $18{:}3_{\Delta 6,9,12}$ bilayer is thinner than that of either $18{:}1_{\Delta 6}$ or $18{:}2_{\Delta 9,12}$, and the pressure profile shows a slightly increased pressure in

TABLE 1 Predicted equilibrium average molecular area (A_{eq}), hydrophobic thickness (H_{eq}), and area elastic modulus (K_a, in units of N/m = 10^3 dyn/cm), for weak ($u_{hg} = 0$) and strong ($u_{hg} = 5$) head group repulsions

	A_{eq} (Å^2)		H_{eq} (Å)		K_a (N/m)	
Lipid chain	$u_{hg} = 5$	$u_{hg} = 0$	$u_{hg} = 5$	$u_{hg} = 0$	$u_{hg} = 5$	$u_{hg} = 0$
14:0	63	57	22.7	25.1	0.22_2	0.21_6
16:0	65	59	24.9	27.3	0.22_3	0.21_6
16:0 + 10% chol	60	55	26.6	29.1	0.23_2	0.22_4
18:0	68	62	26.9	29.3	0.22_4	0.21_7
20:0	70	65	28.9	31.2	0.22_6	0.22_1
$18:1_{\Delta3}$	77	73	23.7	24.9	0.28	0.29
$18:1_{\Delta6}$	77	73	23.7	24.9	0.28	0.30
$18:1_{\Delta9}$	76	72	24.1	25.3	0.29	0.30
$18:1_{\Delta9}$ + 20% chol	65	62	26.3	27.3	0.33	0.35
$18:1_{\Delta12}$	70	66	26.0	27.7	0.27	0.29
$18:1_{\Delta15}$	69	64	26.6	28.7	0.23	0.23
$18:2_{\Delta9,12}$	77	74	23.8	24.7	0.37	0.39
$18:3_{\Delta9,12,15}$	77	74	23.7	24.6	0.36	0.38
$18:3_{\Delta6,9,12}$	85	82	21.6	22.3	0.38	0.40
$20:4_{\Delta5,8,11,14}$	90	88	22.5	23.1	0.39	0.41
$22:6_{\Delta4,7,10,13,16,19}$	96	94	23.3	23.9	0.37	0.38
16:0/$18:1_{\Delta9}$ (equimolar)	71	67	24.2	25.8	0.26	0.27
16:0/$18:1_{\Delta9}$ + 20% chol	60	57	27.1	28.4	0.30_5	0.32
16:0/22:6 (equimolar)	83	80	23.3	24.1	0.34	0.37
16:0/22:6 + 20% chol	73	71	24.6	25.2	0.40	0.42

the layers near the aqueous interface without the decrease in pressure closer to the center of the bilayer that is predicted for $18:1_{\Delta6}$. If it is important to increase the lateral pressure closer to the aqueous interface with a smooth decrease in pressure toward the center of the bilayer, it would appear that multiple unsaturation is effective, although it is accompanied by pronounced thinning of the membrane. Is there a way to effect this shift of pressure out of the bilayer interior without further membrane thinning? Because increasing chain length causes the bilayer to thicken, it seems logical to consider longer multiply unsaturated chains, such as the common membrane lipids formed from arachidonic (20:4) and docosahexaenoic (22:6) acid. In Fig. 2*c*, the pressure profiles predicted for these two lipid chains exhibit a further shift to higher pressures even closer to the aqueous interface, as compared to $18:3_{\Delta6,9,12}$. (The apparent roughness of the pressure profiles, particularly for 22:6, is largely an artifact of the discreteness of the lattice model. In fact, an equimolar mixture of 20:4 and 22:6 gives a much smoother pressure profile of similar overall shape.) Although the thickness of the membrane is much less than that for the saturated chains of biological importance (16:0 and 18:0), it is somewhat greater than that of $18:3_{\Delta6,9,12}$.

Calculations for all of the lipids described above have also been performed over a range of head group repulsion strengths. All else being equal, setting $u_{hg} > 0$ causes a shift in the equilibrium to larger molecular areas, and thus the equilibrium bilayer thickness decreases. However, because $\pi_{hg} = u_{hg}a^{-2}$, bilayers with small molecular area in the absence of head group repulsions, as for saturated chains, are much more strongly affected by incorporation of head group repulsions than those of large molecular area, characteristic of the longer, more highly unsaturated chains, as is clear from the data presented in Table 1. For example, increasing u_{hg} from 0 to 5 (roughly equivalent to switching from PE to PC headgroups at 25°C) results in a decrease in bilayer thickness that is four times greater for the saturated chains than for 20:4 or 22:6.

Lipid mixtures

It is useful to compare the effects of addition of small amounts of various lipid chains and cholesterol with a bilayer of "standard" composition, somewhat arbitrarily chosen to consist of 16:0 chains. Predicted changes in the pressure profile, $\Delta p(z)$, upon addition of 1 mol % of lipids (containing 18:0, 18:1, 18:2, α-18:3, γ-18:3, 20:4, or 22:6 chains) or cholesterol are presented in Fig. 3. Results for both strongly repulsive ($u_{hg} = 5$) and noninteracting ($u_{hg} = 0$) head groups are given. As with the trends for pure lipid bilayers, the addition of unsaturated chains redistributes pressures from a broad region fairly close to the center of the bilayer to a region centered perhaps 4 or 5 Å from the aqueous interface, with little change adjacent to the aqueous interface. The effect is far more pronounced (and the pressure increase is somewhat closer to the interface) for chains with multiple unsaturation beginning near the head groups (γ-18:3, 20:4, 22:6) than for chains with unsaturation no closer than midway down the chain (α-18:3, 18:2, 18:1). For the unsaturated chains, the presence of head group repulsions reduces significantly the magnitude of the pressure changes. Clearly, the effect of cholesterol is unlike that of the unsaturated chains. A pressure decrease is predicted near the interface of greatest magnitude adjacent thereto, with

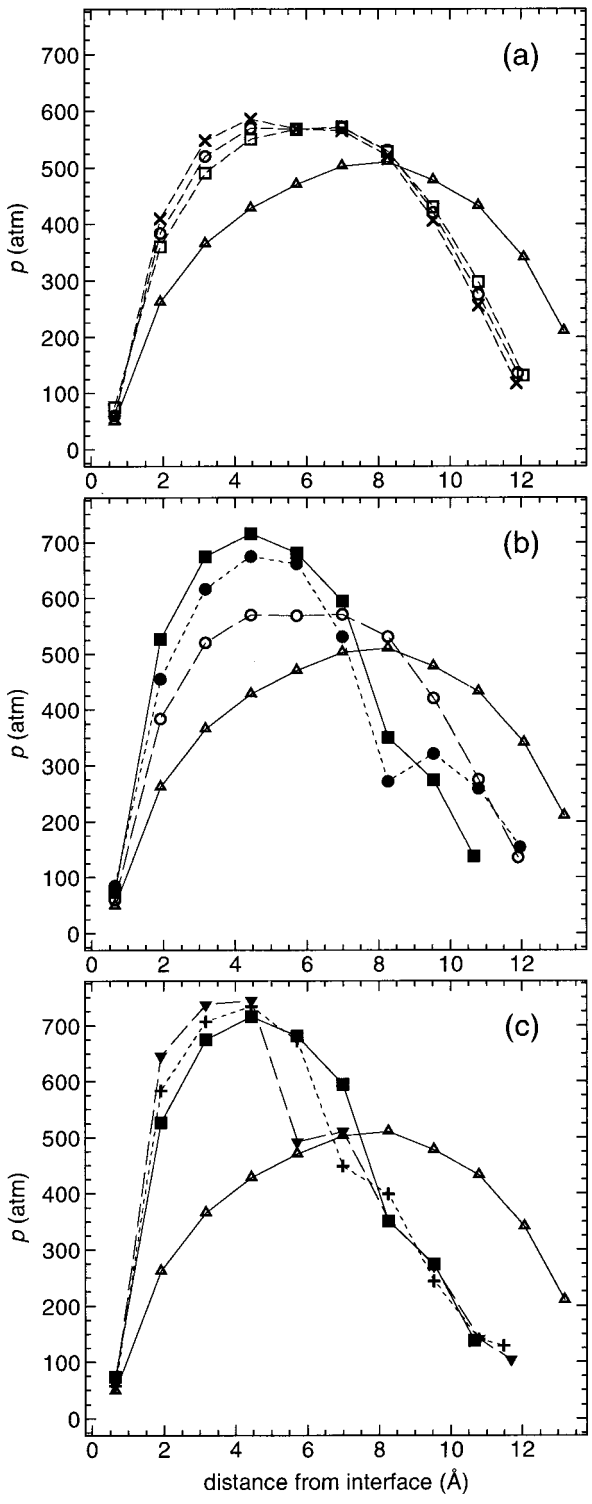

FIGURE 2 Effect on $p(z)$ of increasing acyl chain unsaturation for single-component bilayers without head group repulsions: (□) $18{:}1_{\Delta 9}$; (○) $18{:}2_{\Delta 9,12}$; (×) $18{:}3_{\Delta 9,12,15}$; (●) $18{:}1_{\Delta 6}$; (■) $18{:}3_{\Delta 6,9,12}$; (+) $20{:}4_{\Delta 5,8,11,14}$; (▼) $22{:}6_{\Delta 4,7,10,13,16,19}$; (△) 16:0 (included for purposes of comparison.) All panels are interfacially aligned.

compensating pressure increase in the bilayer interior. Interestingly, the depth at which Δp switches sign is approximately the same as for the highly unsaturated chains.

The admixture of cholesterol or a different lipid to the 16:0 bilayer is accompanied by a change in thickness, as summarized in Table 2. The effect is large and positive for cholesterol while quite negative for the highly unsaturated chains, particularly in the absence of head group interactions. The magnitudes are predicted to be much larger than would result from ideal mixing, as reflected in the calculated partial molar thickness of the added lipid $H_2 = H_{eq} - x_1(dH_{eq}/dx_1)$, in which x_1 is the mole fraction of the majority (16:0) lipid component.

Not surprisingly, the predicted effects of admixture of different lipids are not linear functions of their concentration. In general, the addition of a small amount of saturated chains to a bilayer consisting of unsaturated chains has much smaller impact than a small amount of unsaturated chains added to a saturated bilayer. For example, the pressure profile and thickness of a 1:1 mixture of 16:0 and 18:1 chains are predicted to resemble more closely a bilayer comprised entirely of 18:1 than of 16:0. Also, the shift in the pressure profile accompanying addition of cholesterol becomes increasingly nonlinear for $x_{chol} > 10\%$ (the details depending on the composition of the bilayer to which it is added) even ignoring the possibility of bulk phase separation (Cantor, 1996).

The data presented in Tables 1 and 2 suggest that a wide range of possible manipulations of bilayer composition (such as addition of cholesterol or a shift to weaker headgroup interactions (e.g., PC to PE), accompanied by admixture of either shorter or more unsaturated chains) can leave the membrane thickness unchanged, while significantly redistributing the lateral pressures. The predicted pressure redistributions, $\Delta p(z)$, for some representative compositional changes that conserve thickness are presented in Fig. 4. For example, starting with a bilayer comprised of saturated 16:0 chains, addition of 40 mol % (total) of a mixture of 18:0 and $18{:}1_{\Delta 9}$ lipids is predicted to maintain constant thickness with 25% 18:0 and 15% $18{:}1_{\Delta 9}$ for $u_{hg} = 0$, and with 16.5% 18:0 and 23.5% $18{:}1_{\Delta 9}$ for $u_{hg} = 5$. In both cases, the pressure is redistributed from deep in the membrane interior to a broad region centered about 4 Å from the interface. Pressure redistributions of much greater magnitude are predicted to occur with admixture of cholesterol and highly unsaturated lipids. For example, starting with a bilayer comprised of a 1:1 mix of 16:0 and $18{:}1_{\Delta 9}$ lipids, addition of cholesterol and 20:4 and 22:6 lipids (with a total of 40 mol % of additives, the 20:4 and 22:6 lipids kept in 1:1 proportion) results in no change in thickness for the following compositions: $x_{chol} = 0.18$, $x_{20:4} = x_{22:6} = 0.11$ ($u_{hg} = 0$), and $x_{chol} = 0.12$, $x_{20:4} = x_{22:6} = 0.14$ ($u_{hg} = 5$). The pressure is predicted to decrease immediately adjacent to the aqueous interface, then increases significantly over the next 4 Å, and decreases slightly over the middle half of the bilayer. As a final and somewhat extreme example, weak ($u_{hg} = 0$) head group repulsions are replaced by strong ($u_{hg} = 5$) repulsions for a 1:1 mix of 16:0 and $18{:}1_{\Delta 9}$ lipids (e.g., replacing 1-palmitoyl-2-oleoylphosphatidylethanolamine (POPE) with 1-palmitoyl-2-oleoylphosphatidylcho-

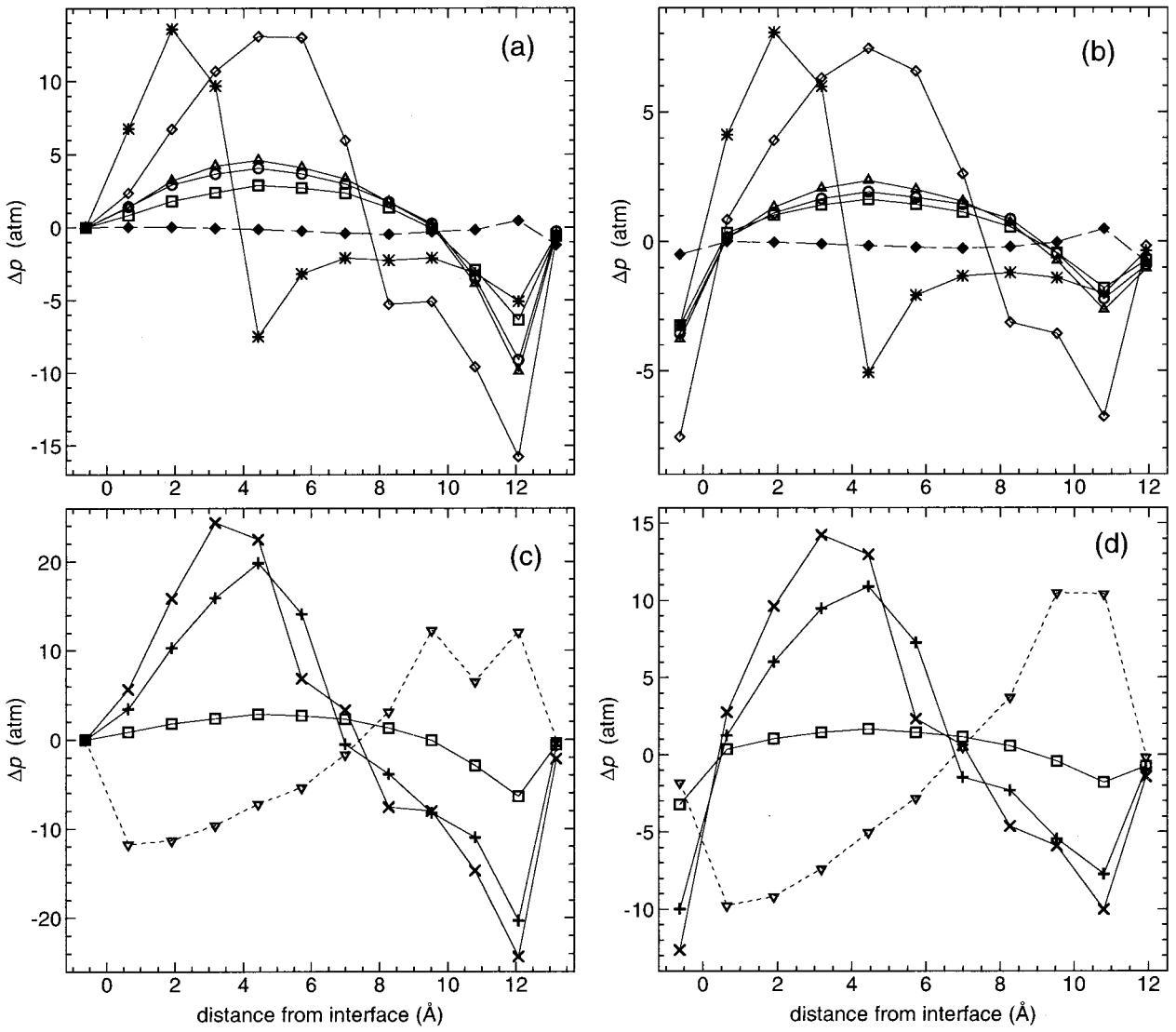

FIGURE 3 Lipid mixtures: $\Delta p(z)$ upon addition of 1 mol % lipid to a 16:0 bilayer. In panels (*a*) and (*c*) the lipids have $u_{hg} = 0$; in (*b*) and (*d*) the lipids (but not cholesterol) have $u_{hg} = 5$. The points at (somewhat arbitrarily placed) negative distance from the interface represent Δp from head group interactions. Additives: (♦) 18:0; (□) $18{:}1_{\Delta 9}$; (○) $18{:}2_{\Delta 9,12}$; (△) $18{:}3_{\Delta 9,12,15}$; (◇) $18{:}3_{\Delta 6,9,12}$; (✳) $18{:}1_{\Delta 3}$; (+) $20{:}4_{\Delta 5,8,11,14}$; (×) $22{:}6_{\Delta 4,7,10,13,16,19}$; (▽) cholesterol. Note the differences in vertical scales.

line (POPC)) and the thickness of the bilayer restored either by addition of cholesterol (12%) or by addition of 18:0 lipid chains (58%). In both cases, the enormous increase in pressure in the head group region is offset by a decrease in pressure spread throughout the bilayer interior. However, with cholesterol, the drop in pressure is greatest near the aqueous interface, whereas with addition of 18:0, the drop is largest at much greater depth within the bilayer. It is evident from the curves in Fig. 4 that changes in the composition of membranes can result in large redistributions of $p(z)$ with no change in thickness, i.e., with no effect on hydrophobic matching.

In an earlier study (Cantor, 1997a), we considered the effect of admixture of short *n*-alkanols on the pressure profile. The predictions obtained in the present analysis resemble qualitatively those obtained earlier. Examples of the resulting $\Delta p(z)$ are presented in Fig. 5*a* for admixture of 1 mol % of alkanol chains of varying length *n* to a bilayer comprised of 16:0 chains with $u_{hg} = 0$ (DPPE). Tethering a short alcohol at one end to the interface requires its volume to be localized near the interface where the pressure increases markedly, compensated by a decrease in pressure spread through the bilayer interior. The spacial localization and thus the magnitude of the effect clearly increase sharply with the difference in lipid and alkanol chain lengths.

Can the effect of short alcohols on $p(z)$ be reproduced using a lipid instead of a small amphiphilic solute? Examination of $p(z)$ for $18{:}1_{\Delta 3}$ as presented in Fig. 1 suggests that a lipid rigidly bent near the head group might act similarly. In Fig. 5*b*, are presented the calculated $\Delta p(z)$ for admixture of 1 mol % of lipids with $18{:}1_{\Delta m}$ chains, for representative small values of *m*. The similarity of the effect of addition of

TABLE 2 Predicted changes in thickness ΔH_{eq} upon addition of 1.0 mol % lipid to a 16:0 bilayer and corresponding partial molar thickness H_2

Added lipid chains	ΔH_{eq} (Å)		H_2 (Å)	
	$u_{hg} = 5$	$u_{hg} = 0$	$u_{hg} = 5$	$u_{hg} = 0$
16:0	0	0	24.9	27.3
18:0	0.023	0.024	27.2	29.7
$18:1_{\Delta 9}$	−0.023	−0.057	22.6	21.6
$18:2_{\Delta 9,12}$	−0.028	−0.098	22.1	17.5
$18:3_{\Delta 9,12,15}$	−0.032	−0.105	21.7	16.8
$18:3_{\Delta 6,9,12}$	−0.095	−0.191	15.4	8.3
$20:4_{\Delta 5,8,11,14}$	−0.105	−0.234	14.4	4.0
$22:6_{\Delta 4,7,10,13,16,19}$	−0.118	−0.273	13.1	0.0
Cholesterol	0.158	0.154	40.7	42.7

small amounts of $18:1_{\Delta m}$ lipids and alkanols of length $n = m$ is striking but not surprising. In both cases, the additive excludes a greater volume close to the interface, either because of its short length or because of the localized *cis*-unsaturation.

The mechanisms by which small interfacially active solutes such as ethanol or general anesthetics modulate the behavior of ion-channel proteins are of enormous interest. Although consideration of nonspecific, lipid-mediated mechanisms is currently unpopular, the redistribution of lateral pressures offers a plausible mechanism for the influence of anesthetics and alcohol on membrane proteins (Cantor, 1997a, 1997b). The results presented in Fig. 5*b*, in which an unnatural lipid and a short *n*-alkanol are predicted to have the same effect on $p(z)$, suggests an unambiguous test of this hypothesis. If it is the redistribution of lateral pressures that results in modulated protein activity, then admixture of an $18:1_{\Delta m}$ lipid into the bilayer should have a similar effect on protein behavior as does introduction of a short alkanol of length $n \approx m$. For ion-channel proteins that can be reconstituted in an artificial bilayer of variable composition, electrophysiological measurements might then provide a test of the relevance of lateral pressure distributions on the mode of action of ethanol and anesthetics.

Molecular areas and area elastic moduli

Molecular areas

As a test of the quality of the approximations intrinsic to the mean-field lattice approach (and the choice of $\omega = 0.45$ as the bending stiffness parameter), we can compare the trends in equilibrium molecular areas reported in Table 1 with experimental measurements and results of molecular dynamics simulations on fully hydrated bilayers. Unfortunately, the results of experimental measurements (Tristram-Nagle et al., 1998; Nagle et al., 1996; Nagle, 1993; Koenig et al., 1997; Rand and Parsegian, 1989) and molecular dynamics simulations (Feller et al., 1997, Tielemann et al., 1997; Tobias et al., 1997) exhibit a considerable range of values of A_{eq} even for the most studied fluid bilayers. Nonetheless, the prediction of a gradual increase of A_{eq} with

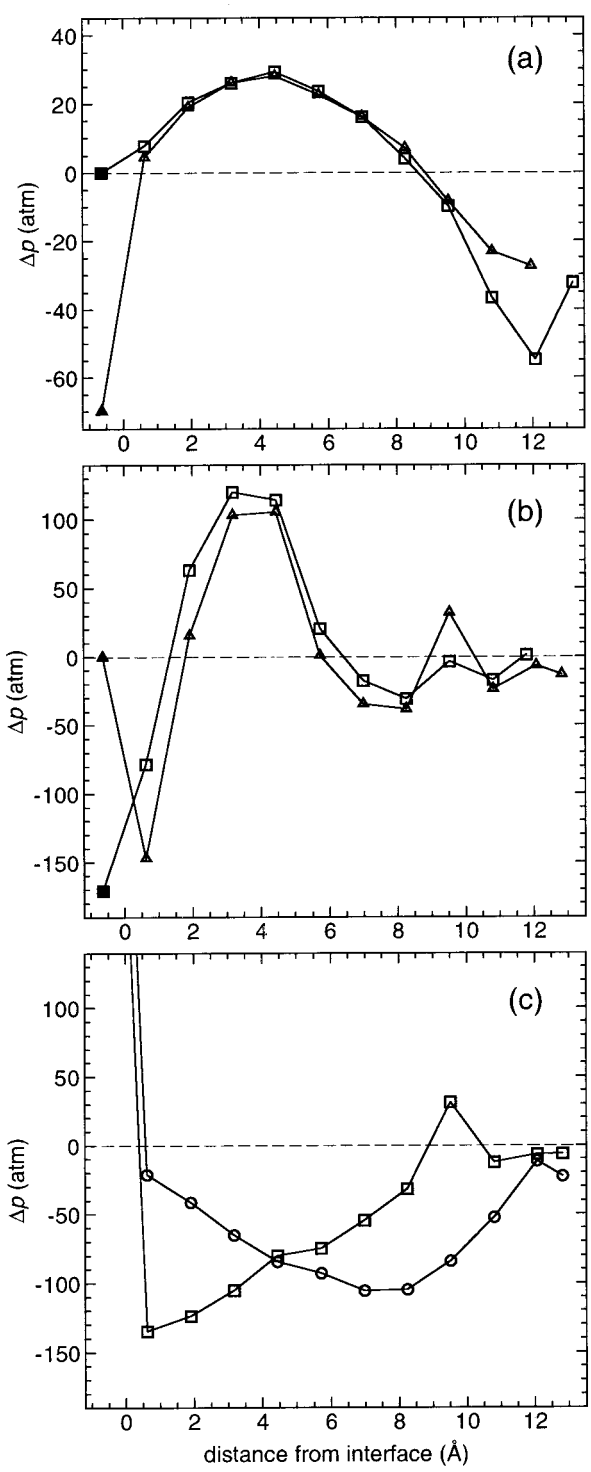

FIGURE 4 $\Delta p(z)$ for multiple changes in lipid composition with composition adjusted to maintain constant thickness. (*a*) 40 mol % (total) of a $18:0/18:1_{\Delta 9}$ mixture added to a 16:0 bilayer. (□) $u_{hg} = 0$; 25% 18:0, 15% $18:1_{\Delta 9}$. (△) $u_{hg} = 5$; 16.5% 18:0, 23.5% $18:1_{\Delta 9}$. (*b*) 40 mol % (total) of a mixture of cholesterol and a 1:1 mixture of 20:4 and 22:6 lipids added to a bilayer comprised of a 1:1 mixture of 16:0 and $18:1_{\Delta 9}$ chains. (□) $u_{hg} = 0$; 11% 20:4, 11% 22:6, 18% cholesterol. (△) $u_{hg} = 5$; 14% 20:4, 14% 22:6, 12% cholesterol. (*c*) To a bilayer comprised of a 1:1 mix of 16:0 and $18:1_{\Delta 9}$ chains, increasing head group repulsion from $u_{hg} = 0$ to $u_{hg} = 5$ occurs at constant thickness either by addition of (□) 12% cholesterol or (○) 58% 18:0 lipid. The accompanying enormous increase in head group repulsion is not shown.

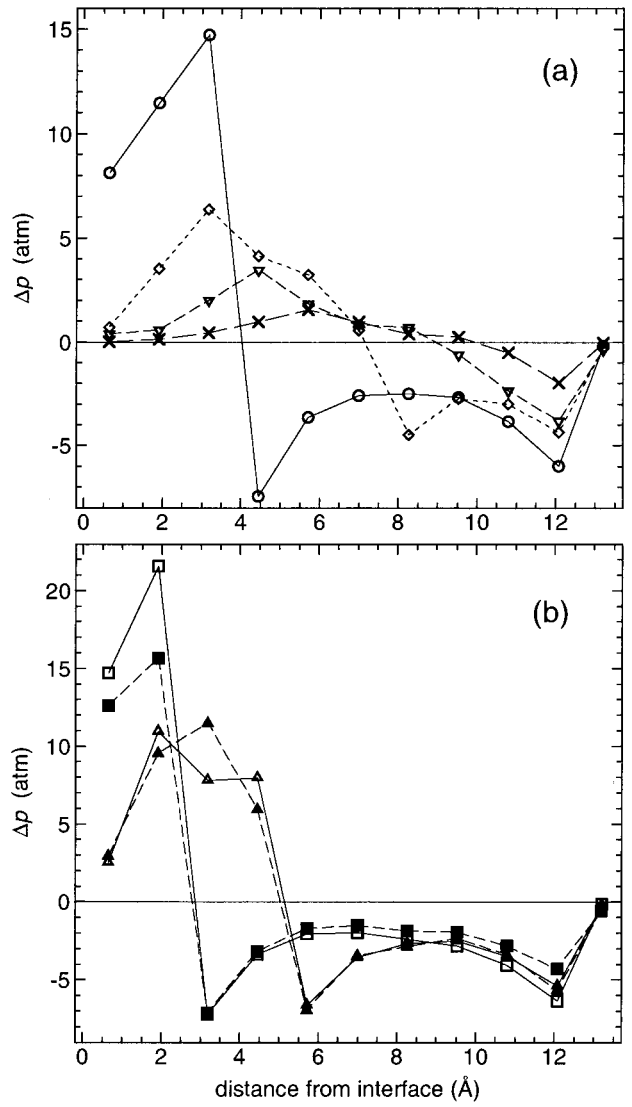

FIGURE 5 (*a*) Change in pressure profile upon addition of 1 mol % alkanol chains to a bilayer comprised of 16:0 chains with $u_{hg} = 0$, for representative alkanol chain lengths: (○) $n = 3$, (◇) $n = 6$, (▽) $n = 9$, (×) $n = 12$. (*b*) Comparison of $\Delta p(z)$ for addition of (*open symbols*) 1 mol % alkanol chains and (*filled symbols*) addition of 1 mol % $18{:}1_{\Delta m}$ lipid chains for $m = n$. Alkanols: (□) $n = 2$; (△) $n = 4$. Lipids: (■) $m = 2$; (▲) $m = 4$.

chain length for saturated chains and with the degree of unsaturation is at least qualitatively consistent with most experimental results. A comparison of dipalmitoylphosphatidylcholine (DPPC) and dioleoylphosphatidylcholine (DOPC) serves as a good example: Tristram-Nagle et al. (1998) and Nagle et al. (1996) report an increase of 9.3 Å^2 (from 62.9 to 72.2 Å^2), whereas an increase of 10.4 Å^2 is predicted in our calculations.

Area elastic moduli

As described earlier, the calculational procedure in the lattice model yields predictions of the free energy over a (discrete) set of values of molecular area bracketing the free energy minimum. From the fit of these points to a continuous curve (from which values of A_{eq} and F_{eq} are obtained), it is possible to evaluate the second areal derivative of the free energy of the bilayer ($F' = 2F$), and thus predict the area elastic modulus

$$K_a = A^{-1}(d^2F'/dA^2) = (2k_BT/A_0)a^{-1}(d^2f/da^2)$$

In most cases, the quality of the fits of f to polynomials in either a or $\ln(a)$ is good enough that the predicted second derivative is virtually unaffected by the choice of fitting procedure (as for saturated chains), although for other lipids (particularly for single-component bilayers comprised of either $18{:}1_{\Delta 9}$, 20:4, or 22:6 chains) the magnification of error that characterizes multiple differentiation does lead to some variability in the predicted values of K_a (the worst case being no more than ± 5%.) More importantly, the predictions for K_a are considerably more sensitive than the pressure profiles to the choice of the chain bending stiffness parameter, the manner in which the *cis*-unsaturation is described, and various other approximations of the lattice mean-field approach. Thus, the values of K_a listed in Table 1 are only useful in revealing qualitative trends (with increasing chain length, unsaturation, cholesterol content, etc.) and would not be expected to provide accurate absolute numerical values. With this caveat in mind, it is still useful to examine the predictions and compare them to measurements from the literature. The lowest values of K_a are predicted for saturated chains, with virtually no dependence on chain length. Addition of one *cis*-unsaturation causes a marked increase in K_a except when the double bond is located near the terminal methyl group of the acyl chain. Increased unsaturation of the acyl chains is predicted to result in even stiffer bilayers. For equimolar mixtures of saturated and unsaturated chains, K_a is calculated to be closer to the value for the pure unsaturated than for the pure saturated system, i.e., the addition of unsaturated chains stiffens the bilayer to a greater degree than a linear relation would predict. Changing the strength of head group repulsions is predicted to have relatively little effect on K_a.

Some, but not all of these trends are observed experimentally (although in general, the predicted K_a are significantly greater than the measured values.) The area elastic modulus of fluid bilayers has been measured using both micropipette suction on vesicles (Evans and Rawicz, 1990; Needham and Nunn, 1990) and obtained using nuclear magnetic resonance and x-ray diffraction on multilamellar dispersions (Koenig et al., 1997) for lipids with varying chain length and unsaturation: diarachidoylphosphatidylcholine (DAPC, di-20:4), dimyristoylphosphatidylcholine (DMPC, di-14:0), 1-stearoyl-2-oleoylphosphatidylcholine (SOPC, $18{:}0/18{:}1_{\Delta 9}$), and 1-stearoyl-2-docosahexaenoylphosphatidylcholine (SDPC, 18:0/22:6). The reported value of K_a is smaller for DMPC bilayers (≈0.14 N/m) than for SOPC bilayers (0.22 N/m at 30°C (Koenig et al., 1997), and 0.19 at 18°C (Evans and Rawicz, 1990) and at 15°C (Needham and Nunn, 1990))

in qualitative agreement with predictions for these lipids (0.22 and 0.26 N/m, respectively). However, whereas K_a is predicted to be even larger for the more highly unsaturated lipids DAPC and SDPC than for SOPC, the measured values are considerably lower: 0.12 N/m (Koenig et al., 1997) for SDPC; 0.14 N/m (Evans and Rawicz, 1990) and 0.06 N/m (Needham and Nunn, 1990) for DAPC. The source of this major discrepancy is not known.

Calculations have been performed for lipid-cholesterol mixtures for a range of cholesterol mole fraction (up to $x_{chol} \approx 0.20$) for a wide range of lipids. For all lipids studied, addition of cholesterol is predicted to result in a gradual increase in K_a, a few examples of which are presented in Table 1. Upon addition of 20% cholesterol, K_a increases by 10 to 20%, the smallest change occuring for saturated lipids. This increase is consistent with measured values for SOPC (Needham and Nunn, 1990) at low cholesterol content. Calculations have not been performed for much higher cholesterol mole fractions, because the theoretical approach presumes the bilayer to remain as a single fluid phase, which is not likely to be the equilibrium state of the bilayer except at fairly low cholesterol content.

DISCUSSION

Lattice statistical thermodynamic methodology based on previous studies on spread monolayer films has been developed and used to calculate the equilibrium distribution of lateral stresses in bilayers. Variation of acyl chain length, the location and number of *cis*-double bonds, the addition of cholesterol and small interfacially active solutes, and variation of the strength of head group repulsions are all predicted to have significant effects both on the pressure profile and on bilayer thickness. To eliminate possible effects of hydrophobic mismatch arising from altered bilayer thickness, changes in bilayer composition were investigated that are predicted to occur at fixed bilayer thickness while effecting a significant redistribution of the pressures.

It would be useful to compare the pressure profiles predicted here with experimental measurements, but no direct and unambiguous measurement of $\pi(z)$ is yet available. In recent studies, using both a mean-field lattice approach and Monte Carlo simulations, Harris and Ben-Shaul (1997) have calculated pressure profiles for bilayers of 5- and 10-segment chains of hard spheres. In their approach, the bonds are of fixed length, and there is no energy dependence of bond angles, except as arises through excluded volume repulsions among nonbonded spheres. The shape of the predicted $\pi(z)$ for saturated chains in Fig. 1*a* and *b* is in qualitative agreement with the results of Harris and Ben-Shaul, although their predicted pressure profile is shifted considerably away from the bilayer interior. This is not surprising, because our calculations are performed for semiflexible chains ($\omega = 0.45$); in fact, results for flexible chains ($\omega = 1.0$, not shown) are in somewhat closer agreement with the predictions of Harris and Ben-Shaul.

The effect of unsaturation on the pressure profile is predicted to be greatest when closest to the head group, because the resulting "kink" is necessarily localized near the aqueous interface where it strongly perturbs the packing of the chains that are quite orientationally ordered in that region, causing a significant increase in lateral pressure at that depth. However, when the double bond occurs toward the end of the acyl chain, it is located predominantly near the center of the membrane where the hydrocarbon chains are orientationally disordered, and thus has relatively little effect on chain packing. For example, lipids derived from two of the commonly occuring unsaturated fatty acids, oleic and linoleic, and the less common α-linolenic acid have very similar effects on the pressure distribution and on bilayer thickness. For all three, the double bond closest to the head group occurs at the ninth carbon with the additional double bonds at the 12-position and the 15-position having little additive effect. Shifting the unsaturation closer to the head groups has an enormous impact as seen in a comparison of α-linolenic and γ-linolenic chains. If a large and broad redistribution of pressure from the interior toward the aqueous interface were needed for proper protein function, it would require lipids with multiple unsaturation beginning closer to the head group and continuing well down the lipid chain. Why then are γ-linolenic chains, which accomplish this objective, not commonly found in membranes? Its large shift in pressure toward the aqueous interface is accompanied by a marked decrease in bilayer thickness, which may also influence membrane proteins. However, longer chains of broadly distributed unsaturation, such as in arachidonic and docosahexaenoic acid, compensate considerably for this thinning while effecting a similar shift in the pressure profile. The importance of these highly unsaturated lipids in membranes may thus result from their ability to shift lateral pressure out of the bilayer interior with minimal membrane thinning, potentially relevant to their role in modulation of rhodopsin activity. The effect on the equilibrium between the meta-I and meta-II states of rhodopsin has been determined as a function of acyl chain unsaturation in phosphatidylcholine bilayers (Litman and Mitchell, 1996) and upon addition of alcohols of varying chain length (Mitchell et al., 1996). An increase in meta-II population (rhodopsin activation) is observed either with increasing chain unsaturation (di-14:0 $\rightarrow$ 16:0/20:4 $\rightarrow$ 16:0/22:6 $\rightarrow$ di-20:4 $\rightarrow$ di-22:6) or with addition of short-chain alcohols (but sharply reduced with increasing alkanol chain length) consistent with the similarity of the predicted effects of increased unsaturation and addition of short alcohols on the pressure profile.

What about the role of cholesterol in membranes? The pressure profile is strongly affected by admixture of even small quantities of cholesterol, characterized by a shift of pressure toward the membrane interior with the decrease in pressure of greatest magnitude adjacent to the aqueous interface. Because cholesterol thickens the bilayer, it serves well in combination with unsaturated lipids (or highly repulsive head groups) to redistribute pressures at constant membrane thickness. It is evident that its effect on $p(z)$ near

the aqueous interface is largely opposite to that of short chain alcohols and other interfacially active small solutes such as general anesthetics. This is consistent with the opposing effects of cholesterol and ethanol on various ion channels such as the nicotinic acetylcholine receptor (Rankin et al., 1997) and the calcium-activated potassium channel (Chang et al., 1995; Chu et al., 1998).

It is interesting that the effect of small interfacially active solutes on the pressure profile can be reproduced by admixture of similar concentrations of lipids that, like ethanol, cause a large pressure increase adjacent to the aqueous interface. This can arise from *cis*-unsaturation near the head group, either in an unnatural acyl chain such as $18{:}1_{\Delta m}$ for small *m*, or possibly through a change in the linkage between the head group and the acyl chains if it is kinked, as in plasmalogens (Lohner, 1996), occupies a greater volume, or requires that the orientation of the connection to one or more of the acyl chains lie more in the plane of the bilayer.

REFERENCES

Andersson, A.-S., L. Rilfors, G. Oradd, and G. Lindblom. 1998. Total lipids with short and long acyl chains from acholeplasma form nonlamellar phases. *Biophys. J.* 75:2877–2887.

Ben-Shaul, A. 1995. Molecular theory of lipid-chain packing, elasticity and lipid-protein interaction in lipid bilayers. *In* Structure and Dynamics of Membranes. R. Lipowsky and E. Sackmann, editors. Elsevier/North Holland, Amsterdam. 359–401.

Ben-Shaul, A., and W. M. Gelbart. 1994. Statistical thermodynamics of amphiphile self-assembly: structure and phase transitions in micellar solutions. *In* Micelles, Membranes, Microemulsions, and Monolayers. W. M. Gelbart, A. Ben-Shaul, and D. Roux, editors. Springer-Verlag, New York. 1–104.

Bienvenüe, A., and J. Sainte Marie. 1994. Modulation of protein function by lipids. *Curr. Topics Memb.* 40:319–354.

Bloom, M., E. Evans, and O. G. Mouritsen. 1991. Physical properties of the fluid lipid-bilayer component of cell membranes: a perspective. *Q. Rev. Biophysics.* 24:293–397.

Brown, M. F. 1997. Influence of nonlamellar-forming lipids on rhodopsin. *Curr. Topics Memb.* 44:285–356.

Cantor, R. S. 1993. Statistical thermodynamics of curvature elasticity in surfactant monolayer films: a molecular approach. *J. Chem. Phys.* 99: 7124–7149.

Cantor, R. S. 1995. The stability of bicontinuous microemulsions: a molecular theory of the bending elastic properties of monolyaers comprised of ionic surfactants and nonionic cosurfactants. *J. Chem. Phys.* 103: 4765–4783.

Cantor, R. S. 1996. Theory of lipid monolayers comprised of mixtures of flexible and stiff amphiphiles in athermal solvents: fluid phase coexistence. *J. Chem. Phys.* 104:8082–8095.

Cantor, R. S. 1997a. The lateral pressure profile in membranes: a physical mechanism of general anesthesia. *Biochemistry.* 36:2339–2344.

Cantor, R. S. 1997b. Lateral pressures in cell membranes: a mechanism for modulation of protein function. *J. Phys. Chem. B* 101:1723–1725.

Cantor, R. S., and P. M. McIlroy. 1989. Statistical thermodynamics of monolayers of flexible-chain amphiphiles: adding nearest-neighbor correlations to a Scheutjens-Fleer approach. *J. Chem. Phys.* 91:416–426.

Chang, H. M., R. Reitstetter, R. P. Mason, and R. Gruener. 1995. Attenuation of channel kinetics and conductance by cholesterol: an interpretation using structural stress as a unifying concept. *J. Mem. Biol.* 143: 51–63.

Chu, B., A. M. Dopico, J. R. Lemos, and S. N. Treistman. 1998. Ethanol potentiation of calcium-activated potassium channels reconstituted into planar lipid bilayers. *Mol. Pharm.* 54:397–406.

Dan, N., and S. Safran. 1998. Effect of lipid characteristics on the structure of transmembrane proteins. *Biophys. J.* 75:1410–1414.

deKruijff, B. 1997. Lipid polymorphism and biomembrane function. *Curr. Opin. Chem. Biol.* 1:564–569.

Edidin, M. 1997. Lipid microdomains in cell surface membranes. *Curr. Opin. Struc. Bio.* 7:528–532.

Epand, R. M. 1996. The properties and biological roles of non-lamellar forming lipids. *Chem. Phys. Lipids*. 81:101–264.

Evans, E., and W. Rawicz. 1990. Entropy-driven tension and bending elasticity in condensed-fluid membranes. *Phys. Rev. Lett.* 64: 2094–2097.

Feller, S. E., R. M. Venable, and R. W. Pastor. 1997. Computer simulation of a DPPC phospholipid bilayer: structural changes as a function of molecular surface area. *Langmuir.* 13:6555–6561.

Franks, N. P., and W. R. Lieb. 1994. Molecular and cellular mechanisms of general anesthesia. *Nature.* 367:607–614.

Gruner, S. 1989. Stability of lyotropic phases with curved interfaces. *J. Phys. Chem.* 93:7562–7570.

Gruner, S. 1991. Lipid membrane curvature elasticity and protein function. *In* Biologically Inspired Physics. L. Peliti, editor. Plenum Press, New York. 127–135.

Harris, D., and A. Ben-Shaul. 1997. Conformational chain statistics in a model lipid bilayer: comparison between mean-field and Monte Carlo calculations. *J. Chem. Phys.* 106:1609–1619.

Holopainen, J. M., J. Y. A. Lehtonen, and P. K. J. Kinnunen. 1997. Lipid microdomains in dimyristoylphosphatidylcholine-ceramide liposomes. *Chem. Phys. Lipids.* 88:1–13.

Hui, S. W. 1997. Curvature stress and biomembrane function. *Curr. Topics Memb.* 44:541–563.

Jaycock, J., and G. D. Parfitt. 1981. Chemistry of Interfaces. Wiley, New York.

Keller, S. L., S. M. Bezrukov, S. M. Gruner, M. W. Tate, I. Vodyanoy, and V. A. Parsegian. 1993. Probability of alamethicin conductance states varies with nonlamellar tendency of bilayer phospholipids. *Biophys. J.* 65:23–27.

Koenig, B. W., H. H. Strey, and K. Gawrisch. 1997. Membrane lateral compressibility determined by NMR and x-ray diffraction: effect of acyl chain polyunsaturation. *Biophys. J.* 73:1954–1966.

Leermakers, F. A. M., and J. Lyklema. 1992. On the self-consistent field theory of surfactant micelles. *Colloids Surf.* 67:239–255.

Leermakers, F. A. M., and J. M. H. M. Scheutjens. 1988. Statistical thermodynamics of association colloids: III. The gel to liquid phase transition of lipid bilayer membranes. *J. Chem. Phys.* 89:6912–6924.

Litman, B. J., and D. C. Mitchell. 1996. A role for phospholipid polyunsaturation in modulating membrane protein function. *Lipids.* 31:S193-S197.

Lohner, K. 1996. Is the high propensity of ethanolamine plasmalogens to form non-lamellar lipid structures manifested in the properties of biomembranes? *Chem. Phys. Lipids.* 81:167–184.

Lundbaek, J. A., and O. S. Andersen. 1999. Spring constants for channel-induced lipid bilayer deformations. *Biophys. J.* 76:889–895.

Mitchell, D. C., J. T. R. Lawrence, and B. J. Litman. 1996. Primary alcohols modulate the activation of the G protein-coupled receptor rhodopsin by a lipid-mediated mechanism. *J. Biol. Chem.* 271: 19033–19036.

Merz, K. M., and B. Roux. 1996. Biological Membranes: A Molecular Perspective from Computation and Experiment. Birkhäuser, Boston.

Morein, S., A.-S. Andersson, L. Rilfors, and G. Lindblom. 1996. Wild type *Escherichia coli* cells regulate the membrane lipid composition in a 'window' between gel and non-lamellar structures. *J. Biol. Chem.* 271: 6801–6809.

Mouritsen, O. G., and M. Bloom. 1993. Models of lipid-protein interactions in membranes. *Annu. Rev. Biophys. Biomol. Struct.* 22:145–171.

Mouritsen, O. G., and K. Jørgensen. 1997. Small-scale lipid-membrane structure: simulation versus experiment. *Cur. Opin. Struc. Biol.* 7:518–527.

Nagle, J. F. 1993. Area/lipid of bilayers from NMR. *Biophys. J.* 64: 1476–1481.

Nagle, J. F., R. Zhang, S. Tristram-Nagle, W. Sun, and H. I. Petrache. 1996. X-ray structure determination of fully hydrated L_α phase dipalmitoylphosphatidylcholine bilayers. *Biophys. J.* 70:1419–1431.

Needham, D., and R. S. Nunn. 1990. Elastic deformation and failure of lipid bilayer membranes containing cholesterol. *Biophys. J.* 58: 997–1009.

Nielsen, C., M. Goulian, and O. S. Andersen. 1998. Energetics of inclusion-induced bilayer deformations. *Biophys. J.* 74:1966–1983.

Rand, R. P., and V. A. Parsegian. 1989. Hydration forces between phospholipid bilayers. *Biochim. Biophys. Acta.* 988:351–376.

Rankin, S. E., G. H. Addona, M. A. Kloczewiak, B. Bugge, and K. W. Miller. 1997. The cholesterol dependence of activation and fast desensitization of the nicotinic acetylcholine receptor. *Biophys. J.* 73: 2446–2455.

Seddon, J. M. 1990. Structure of the inverted hexagonal (H_{II}) phase, and non-lamellar phase transitions of lipids. *Biochim. Biophys. Acta.* 1031:1–69.

Stigter, D., J. Mingins, and K. A. Dill. 1992. Phospholipid interactions in model membrane systems. *Biophys. J.* 61:1616–1629.

Tielemann, D. P., S. J. Marrink, and H. J. C. Berendsen. 1997. A computer perspective of membranes: molecular dynamics studies of lipid bilayer systems. *Biochim. Biophys. Acta.* 1331:235–270.

Tobias, D. J., K. Tu, and M. L. Klein. 1997. Atomic-scale molecular dynamics simulations of lipid membranes. *Curr. Opin. Coll. Interface Sci.* 2:15–26.

Tristram-Nagle, S., H. I. Petrache, and J. F. Nagle. 1998. Structure and interactions of fully hydrated dioleoylphosphatidylcholine bilayers. *Biophys. J.* 75:917–925.

Wijmans, C. M., F. A. M. Leermakers, and G. J. Fleer. 1994. Chain stiffness and bond correlations in polymer brushes. *J. Chem. Phys.* 101:8214–8223.